Vol. 46, No. 4 (2024) 549-559, DOI: 10.24874/ti.1660.04.24.05

Tribology in Industry

www.tribology.rs

RESEARCH

# A Study on Material Removal Rate in Powder-Mixed Electro-Discharge Machining Utilizing Integrated Experimental and Computational Fluid Dynamics Analysis

Nguyen Huu-Phan[a], V.S. Ganachari[b], Shailesh Shirguppikar[c], P.B. Gavali[d], S.S. Deshmukh[e], P.S. Jadhav[f], L. Selvarajan[g], Nguyen Duc-Toan[h,*], M.V. Pachore[i]

[a]*Hanoi University of Industry, No. 298, CauDien Street, Bac TuLiem District, Hanoi, Vietnam*,
[b,c,d,e]*Department of Mechatronics Engineering, Rajarambapu Institute of Technology, Shivaji University, Sakharale, MS -414415, India,*
[f]*Department of Mechanical Engineering, Rajarambapu Institute of Technology, Rajaramnagar, Islampur, India,*
[g]*Department of Mechanical Engineering, Mahendra Institute of Technology (Autonomous), Namakkal, 637503, Tamilnadu, India,*
[h]*School of Mechanical Engineering, Ha Noi University of Science and Technology, No 1 Dai Co Viet Stress, Hai Ba Trung District, Ha Noi City, 100000, Vietnam,*
[i]*Research Student, Department of Automation Engineering, University of Bologna, Italy.*

Keywords:

*Powder-mixed electro-discharge Machining*
*Material removal rate*
*Experimental analysis*
*Computational fluid dynamics*
*Machining efficiency*

* Corresponding author:

*Nguyen Duc-Toan*
*E-mail: toan.nguyenduc@hust.edu.vn*

*Received: 12 April 2024*
*Revised: 15 May 2024*
*Accepted: 29 June 2024*

CC BY NC

A B S T R A C T

*Electric discharge machining (EDM) serves as a pivotal technique for the precision machining of materials known for their inherent difficulty in conventional cutting processes. Its capability to fashion blind slots and intricate features in conductive materials, otherwise challenging to fabricate using traditional methods, underscores its significance in modern manufacturing. The effectiveness of Electrical Discharge Machining (EDM) hinges upon a multifaceted interplay of electrical and non-electrical variables, encompassing parameters such as current, voltage, cycle time, and powder concentration. This study delves into the realm of EDM with a specific focus on Powder-Mixed Electro-Discharge Machining (PMEDM), aiming to comprehensively explore and optimize the material removal rate (MRR). The experimental investigation, conducted with and without the incorporation of conductive powder particles into the dielectric medium, scrutinizes the impact on MRR, thereby shedding light on the efficacy of powder integration in enhancing machining efficiency. Furthermore, the study ventures into the realm of computational fluid dynamics (CFD) to simulate and analyze the intricate dynamics of dielectric flow, powder particle behavior, and debris movement within the inter-electrode gap (IEG). These simulations serve as invaluable tools in elucidating the underlying mechanisms governing the machining process, providing insights into the intricate interplay between electrical discharges, fluid flow, and particulate dynamics.*

*The synthesis of experimental data and simulation results reveals a strong correlation between the inclusion of powder particles in the dielectric medium and the enhancement of machining efficiency, particularly evident in the observed improvements in MRR. The consistency between experimental findings and simulation outcomes underscores the validity and robustness of the study's methodologies and conclusions. In essence, this research not only contributes to the advancement of understanding of PMEDM but also underscores the potential of integrated experimental and computational approaches in optimizing machining processes. By elucidating the intricate dynamics of powder-mixed EDM and its implications on material removal efficiency, this study paves the way for enhanced precision machining in various industrial applications*.

© 2024 Published by Faculty of Engineering

## 1. INTRODUCTION

The conventional machining paradigm hinges upon the premise that the tool must be harder than the workpiece. However, the rapid advancements in materials science have presented formidable challenges to this age-old principle, rendering it inadequate for addressing the diverse array of newly developed materials. In response to this machining conundrum, non-conventional machining processes have emerged as promising alternatives, offering innovative solutions to the limitations encountered in traditional methods. Among these, Electrical Discharge Machining (EDM) has garnered widespread acclaim as a highly effective method for machining materials deemed difficult to cut using conventional means.

Despite its widespread adoption, EDM is not without its shortcomings. Issues such as machining efficiency, surface quality, tool wear rate, and low material removal rate (MRR) have persisted, necessitating the exploration of novel approaches to enhance its performance. In this context, the powder-mixed EDM process emerged in the 1980s as a pioneering solution, with researchers directing their efforts towards augmenting machining performance through the incorporation of various conductive powder particles into the dielectric medium. The utilization of powder particles in a dielectric medium has been shown to yield significant improvements in both MRR and surface finish [1-2].

Studies by Surekha et al. have underscored the substantial contributions of powder concentration, current, and gap voltage, attributing a 50% impact on MRR and surface roughness (SR) among other parameters such as cycle time, duty factor, and gap distance [3]. Similarly, investigations by Anand Y. Joshi and Nipun D. Gosai into the effect of silicon carbide powder particles have demonstrated the pivotal role of powder particles in enhancing MRR and surface finish, with silicon powder yielding a remarkable 60% increase in MRR compared to processes without powder particles [4].

Furthermore, the incorporation of surfactant and graphite powder into the dielectric medium has been shown to exert a significant influence on surface finish, particularly in terms of MRR, with current and graphite powder contributing significantly to the development of recast layer thickness on workpiece material [5]. Studies by Shih Ou on the machining of titanium alloy using a mixture of conductive bioceramic particles and dielectric medium have yielded promising results, with significant improvements observed in MRR and surface finish [6].

The efficacy of conductive powder in enhancing MRR and reducing surface roughness has been corroborated by numerous studies, particularly in water-based dielectric mediums, demonstrating an improvement in MRR and a reduction in SR. Notably, the PMEDM process has exhibited superior performance on Metal Matrix Composites (MMCs) compared to conventional machining techniques [7-9].

Moreover, researchers have explored the application of the PMEDM process for machining biomedical implants, revealing precise surface modification facilitated by the use of antibacterial powder in the dielectric medium, surpassing the efficacy of conventional antibacterial coatings [8-10].

In tandem with experimental endeavors, studies utilizing Computational Fluid Dynamics (CFD) techniques, such as those conducted by Mullya and Karthikeyan, have elucidated the intricate dynamics of debris particle behavior in the dielectric medium. These investigations have underscored the significant impact of debris movement on EDM performance, providing valuable insights into the phenomena underlying machining processes [11-13].

This paper provides a comprehensive overview of Powder Mixed Electrical Discharge Machining (PMEDM) and its evolution, juxtaposed with traditional Electrical Discharge Machining (EDM). Key performance metrics such as tool wear rate, material removal rate, and surface roughness are meticulously examined. A detailed comparison between PMEDM and EDM is presented, elucidating the advancements in PMEDM technology [14].

Experimental investigations were conducted to alter the surfaces of Ti6Al4V by introducing silver nanopowder into a hydrocarbon-based dielectric fluid. The objective was to explore the discharge separation mechanism in PMEDM. Analysis focused on surface topography, chemical composition, and the distribution of deposited silver content under various polarities. Additionally, PMEDM and traditional EDM current waveforms were studied across different discharge energies, both with and without ultrasonic vibration assistance. Computational Fluid Dynamics (CFD) simulations were employed to model the dielectric fluid's flow field, facilitating the analysis of nanopowder distribution and velocity within the machining gap with internal flushing. The results suggest that PMEDM holds promise as a technology for concurrently modifying the antibacterial surface of medical devices during milling processes [15].

The study examines the effects of titanium nitride (TiN) coating on tungsten carbide (WC) micro-electrodes during Micro-Electro Discharge Machining (MEDM) of Ti-6Al-4V alloy. The aim of this research is to determine the effect of TiN coating on tool wear rate (TWR), overcut (OC), and depth of machining (Z coordinator) during the micro-drilling process [16-17].

Inspired by these insights, the present study embarks on a comprehensive exploration, adulterating a silicon carbide powder into a dielectric medium to evaluate its effect on MRR and surface quality. Furthermore, CFD simulations will be employed to analyze powder particle and debris trajectory, shedding light on the nuanced interactions shaping EDM performance. Through this integrated approach, the study endeavors to advance our understanding of the intricate dynamics of PMEDM and its implications for machining efficiency and surface quality.

## 2. EXPERIMENT AND SIMULATION

### 2.1 Experimental work

In the current study, the workpiece material selected is AISI D3, characterized by its dimensions of (100x50x10) mm and known as high carbon high chromium tool steel. Renowned for its high wear resistance and compressive strength, AISI D3 presents an ideal candidate for assessing the performance of the powder-mixed Electrical Discharge Machining (PMEDM) process. For tooling purposes, a cylindrical copper bar with a diameter of 10 mm at the spark point and a length of 50 mm is employed.

The experimentation is conducted using a die sinking ZNC EDM machine specifically designed for PMEDM processes. To facilitate the machining process while minimizing dielectric material (EDM-Oil) consumption, a custom tank with dimensions of (450x300x150) mm is fabricated. This tank features a circulation system comprising a stirrer and pump to ensure efficient mixing of silicon carbide powder particles within the dielectric medium, thereby preventing the formation of lumps. The schematic representation of the experimental setup is illustrated in Figure 1.

**Fig. 1.** Experimental setup.

The parameters selected for experimentation include current (I), voltage (V), cycle time (TON), powder concentration (P.C.), and duty factor (D.F.). These parameters are varied across specified levels, as summarized in Table 1, to assess their influence on Material Removal Rate (MRR).

**Table 1.** Parameters range and level.

| Parameters | Levels | | |
|---|---|---|---|
| Current (I(A)) | 2 | 21 | 40 |
| Voltage (U(V)) | 40 | 70 | 100 |
| Cycle time (TON(µsec)) | 50 | 100 | 150 |
| Powder Conc. (P.C. (gm/lit)) | 0 | 2 | 4 |
| Duty Factor (D.F.) | 6 | 9 | 12 |

The experimental design is constructed using the L27 orthogonal array of the Taguchi method in Minitab 19 software. Through systematic experimentation, the machining efficiency is evaluated based on MRR, as outlined in Table 2.

**Table 2.** Experimentation result.

| Expt. No. | I (A) | U (V) | TON (µs) | P.C. (gm/lit) | D.F. | MRR gm/min |
|---|---|---|---|---|---|---|
| 1 | 2 | 40 | 50 | 0 | 6 | 2.15 |
| 2 | 2 | 40 | 100 | 2 | 9 | 3.67 |
| 3 | 2 | 40 | 150 | 4 | 12 | 4.15 |
| 4 | 2 | 70 | 50 | 2 | 12 | 5.26 |
| 5 | 2 | 70 | 100 | 4 | 6 | 8.08 |
| 6 | 2 | 70 | 150 | 0 | 9 | 7.26 |
| 7 | 2 | 100 | 50 | 4 | 9 | 7.47 |
| 8 | 2 | 100 | 100 | 0 | 12 | 7.89 |
| 9 | 2 | 100 | 150 | 2 | 6 | 8.26 |
| 10 | 21 | 40 | 50 | 0 | 6 | 3.14 |
| 11 | 21 | 40 | 100 | 2 | 9 | 3.5 |
| 12 | 21 | 40 | 150 | 4 | 12 | 5.74 |
| 13 | 21 | 70 | 50 | 2 | 12 | 8.58 |
| 14 | 21 | 70 | 100 | 4 | 6 | 9.22 |
| 15 | 21 | 70 | 150 | 0 | 9 | 9.05 |
| 16 | 21 | 100 | 50 | 4 | 9 | 9.72 |
| 17 | 21 | 100 | 100 | 0 | 12 | 10.16 |
| 18 | 21 | 100 | 150 | 2 | 6 | 11.24 |
| 19 | 40 | 40 | 50 | 0 | 6 | 4.05 |
| 20 | 40 | 40 | 100 | 2 | 9 | 4.78 |
| 21 | 40 | 40 | 150 | 4 | 12 | 7.54 |
| 22 | 40 | 70 | 50 | 2 | 12 | 10.63 |
| 23 | 40 | 70 | 100 | 4 | 6 | 10.28 |
| 24 | 40 | 70 | 150 | 0 | 9 | 11.01 |
| 25 | 40 | 100 | 50 | 4 | 9 | 11.96 |
| 26 | 40 | 100 | 100 | 0 | 12 | 10.69 |
| 27 | 40 | 100 | 150 | 2 | 6 | 13.89 |

## 2.2 CFD modelling

In the PMEDM process, the tool remains stationary, creating a blind hole in the workpiece. The diameter of this hole is contingent upon the tool diameter and inter-electrode gap (IEG), which is maintained at 2 mm. A stirrer mechanism is employed to flush debris particles from the IEG, thereby preventing arcing and secondary discharge, ultimately enhancing machining efficiency.

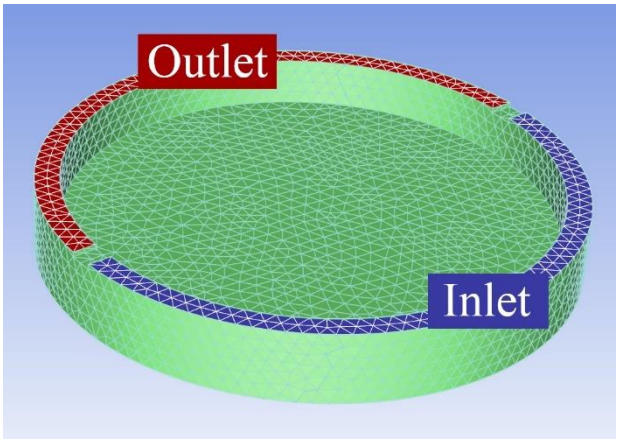


**Fig. 2.** Workpiece 3D model for simulation.

For CFD simulations, the workpiece is modeled in 3D, as depicted in Figure 2. The simulation entails maintaining a 2 mm IEG between the workpiece and electrode, with inlet and outlet positions strategically placed to mimic the flushing mechanism. Although these inlet and outlet points are not present in the actual machining process, their inclusion facilitates the simulation of debris particle movement.

Figure 2 depicts the fluid domain filled with kerosene, a dielectric. To maintain an adequate quantity of dielectric within the gap, it is introduced through the inlet cross-section, with the excess dielectric exiting through the outlet cross-section after circulating through the inter-electrode gap (IEG). The simulation model includes a wall to distinguish the inlet from the outlet cross-sections, though this wall does not affect the flow field at the outlet.

To evaluate the effectiveness of the flushing process, spherical steel particles are injected from the workpiece surface, and their movement through the IEG is tracked. The Euler-Lagrange approach is employed to monitor these particles (discrete phase), using

one-way coupling due to the relatively low volume of particles compared to the dielectric (continuous phase). The Schiller-Naumann drag model is used to calculate momentum transfer between the fluid and the particles. The computational fluid dynamics (CFD) parameters used for simulating fluid flow and discrete phase modeling are detailed in Table 3.

**Table 3.** Boundary conditions for the simulation.

| | |
|---|---|
| Solver class | 3D modelling using pressure calculations, with high precision and without considering the effects of gravity. |
| Class of simulation | Equilibrium state Calculation. |
| Velocity expression | Absolute |
| Gradient option | Least squares cell based |
| Turbulence class | Implementable k–e turbulence model with conventional wall functions |
| Topics are momentum, turbulence, dissipation rate, and energy discretization methods | Second order up winding |
| Pressure–velocity coupling | SIMPLE |
| Criteria for residual | 10-3 for continuity, velocities, k and e, 10-6 for energy |
| Meshing class | triangle elements |

Several assumptions are made for the simulation: the effect of gravity on the particles is neglected; the impact of particles on the dielectric fluid flow is disregarded due to their low quantity; and a no-slip condition is applied to the workpiece surfaces. The simulation parameters, outlined in Table 3, are configured to model the flow behavior and trajectory of powder and debris particles within the dielectric medium. The workpiece is meshed with triangular elements to facilitate the simulation of debris particle evacuation.

**Table 4.** DPM parameters used for simulation.

| | |
|---|---|
| Particle treatment | Steady particle tracking |
| Drag law | Spherical |
| Physical models | Erosion/accretion |
| Gradient option | Least squares cell based |
| Turbulent dispersion | Cloud tracking |
| Injection type | Surface |
| Particle type | Inert, uniform diameter distribution |

Furthermore, the discrete phase modeling (DPM) method is used to study particle trajectories within the gap. Implemented using the Euler-Lagrange model in ANSYS FLUENT, the DPM model tracks multiple particles as the secondary phase interacting with the primary fluid phase (EDM oil). Spherical metal particles with diameters of 5, 10, and 14 μm are utilized to represent powder particles in the simulation. Table 4 summarizes the parameters used for the DPM simulation.

Numerical methods play a pivotal role in solving the Navier-Stokes equations, which are fundamental in understanding and predicting fluid flow phenomena. Equation (1), governing the motion of fluid substances, is expressed as:

$$p\left(\frac{\delta y}{\delta x}+u\frac{\delta y}{\delta x}+v\frac{\delta y}{\delta x}+w\frac{\delta y}{\delta x}\right)=p.\mathrm{gx}-\frac{\delta p}{\delta x}+\mu\left(\frac{d^2u}{dx^2}+\frac{d^2u}{dy^2}+\frac{d^2u}{dz^2}\right) \quad (1)$$

Here, ρ signifies the density of the fluid medium, with u, v, and w representing the velocity components along the Cartesian coordinates of the x, y, and z axes, respectively. Additionally, g denotes the gravitational acceleration experienced by the fluid, while p denotes the pressure exerted within the fluid domain. Furthermore, μ symbolizes the dynamic viscosity of the fluid, representing its resistance to shear deformation under applied stress.

This equation is indispensable in studying fluid dynamics across various fields, including aerospace engineering, environmental science, and biomedical engineering. By discretizing these equations on a computational mesh, numerical methods enable the calculation of fluid flow characteristics and properties. The discretization process involves dividing the fluid domain into small elements or cells, allowing for the approximation of fluid behavior within each cell.

Through computational fluid dynamics (CFD) simulations, numerical methods facilitate the analysis of complex fluid flow phenomena, such as turbulence, boundary layer separation, and vortical structures. Researchers can employ advanced numerical techniques, such as finite volume, finite element, or finite difference methods, to solve the discretized equations iteratively over the computational domain.

Furthermore, numerical simulations offer researchers the flexibility to explore various boundary conditions, geometries, and operating parameters, providing valuable insights into fluid behavior under different scenarios. These simulations help optimize engineering designs, predict performance characteristics, and guide decision-making processes in fluid-related applications. Numerical methods serve as indispensable tools for solving the Navier-Stokes equations and studying fluid flow behavior. Their application in computational fluid dynamics enables to gain deeper insights into complex fluid phenomena, ultimately contributing to advancements in engineering, science, and technology.

Through this integrated experimental and computational approach, the study aims to elucidate the intricate dynamics of the PMEDM process, providing valuable insights into its performance and shedding light on avenues for optimization and improvement.

## 3. RESULTS AND DISCUSSION

### 3.1 Effect of electrical parameters on MRR

The experimental investigation, utilizing the Taguchi experimental design method and the L27 orthogonal array, focuses on analyzing the impact of electrical parameters on Material Removal Rate (MRR) in powder-mixed Electrical Discharge Machining (PMEDM). Specifically, the study evaluates the influence of four electrical parameters - current, voltage, cycle time (TON), and duty factor - along with powder concentration (P.C.) on MRR.

Incorporating conductive powder particles into the dielectric medium introduces alterations in the electrical characteristics of the machining environment. This inclusion decreases the dielectric's breakdown strength while concurrently augmenting the inter-electrode gap (IEG), thereby facilitating a more efficient machining process by renovating the workpiece surface and averting arcing. The charged particles within the gap undergo acceleration and exhibit a zigzag trajectory, contributing to stable sparking and ultimately enhancing the MRR.

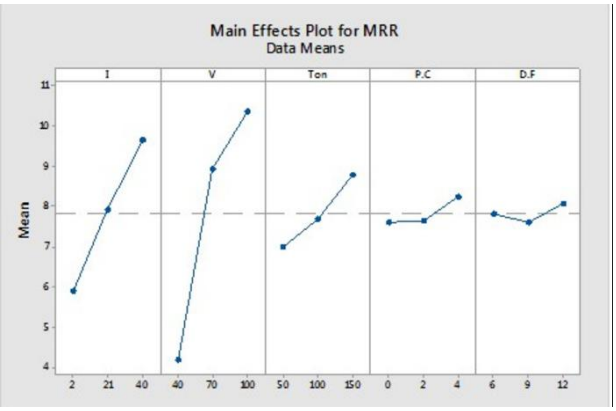


**Fig. 3.** Main effects plot of MRR.

Figure 3 illustrates the behavior of various parameter ranges on MRR. The primary power sources, current, and voltage demonstrate a significant influence on MRR, with an observable improvement as their values increase. This linear improvement can be attributed to the enhanced spark energy within the IEG, leading to elevated temperatures in the machining zone. Additionally, an increase in powder concentration beyond 2 gm/lit results in a notable enhancement of MRR, facilitating the formation of a stable sparking zone and robust plasma channel within the IEG. However, the duty factor exhibits a comparatively minor effect on MRR.

### 3.2 ANOVA analysis

The analysis of variance (ANOVA) method is employed to scrutinize the experimental data, providing insights into the significance of each parameter on MRR. Table 5 presents a summary of the ANOVA results, indicating the parameters' degrees of freedom (DF), sum of squares (SS), mean squares (MS), F-values, P-values, and their respective contributions to MRR.

The ANOVA results highlight the particular significance of current, voltage, and cycle time (TON), as evidenced by their associated P-values falling below the 0.05 threshold. These parameters exhibit substantial contributions to MRR, with voltage accounting for 67.57% and current contributing 22.91%. Conversely, powder concentration and duty factor demonstrate lesser contributions to MRR. The acceptable error percentage further validates the ANOVA results.

**Table 5.** ANOVA of MRR.

| Parameters | DF | SS | MS | F | P | Contribution |
|---|---|---|---|---|---|---|
| Current | 2 | 63.18 | 31.5 | 56.3 | 0.000 | 22.71 |
| Voltage | 2 | 187.9 | 93.9 | 167.6 | 0.000 | 67.57 |
| Cycle On Time | 2 | 14.87 | 7.43 | 13.2 | 0.000 | 5.346 |
| Powder Concentration | 2 | 2.272 | 1.13 | 2.03 | 0.164 | 0.816 |
| Duty Factor | 2 | 0.970 | 0.48 | 0.87 | 0.440 | 0.348 |
| Error | 16 | 8.969 | 0.56 | | | 3.223 |
| Total | 26 | 278.2 | | | | |
| S = 0.748710 R-Sq = 96.78% R-Sq(adj) = 94.76% | | | | | | |

### 3.3 Effect of powder particles on MRR by simulation

The application of voltage between electrodes in Electrical Discharge Machining (EDM) initiates an electric field, leading to an increased gap distance between the tool and workpiece. As the spark gap becomes filled with more powder particles, their energization and subsequent zigzag motion contribute to stable sparking, thereby enhancing Material Removal Rate (MRR). This process is vividly depicted in Figure 4, where (a) illustrates the erosion rate without silicon carbide, and (b) showcases the erosion rate with silicon carbide, highlighting the enhanced crater generation due to stable discharge facilitated by powder particles.

Figure 4a portrays the erosion rate in a scenario devoid of silicon carbide particles within the dielectric medium. This configuration reflects a conventional EDM setup, where the machining process relies solely on the electrical discharge between the electrode and the workpiece. In the absence of silicon carbide, the discharge phenomena exhibit relatively erratic behavior, leading to irregular material removal patterns and inconsistent surface erosion. Consequently, machining efficiency and surface finish may suffer, hindering the achievement of desired machining outcomes.

In contrast, Figure 4b demonstrates the erosion rate with the inclusion of silicon carbide particles extensively within the dielectric medium. The incorporation of silicon carbide confers several notable advantages to the EDM process, mainly by enhancing the stability and efficacy of electrical discharge phenomena. With silicon carbide particles present, the discharge process becomes more controlled and uniform, resulting in smoother material removal and more predictable surface erosion patterns. Consequently, machining efficiency is markedly improved, accompanied by enhancements in surface finish quality and dimensional accuracy.

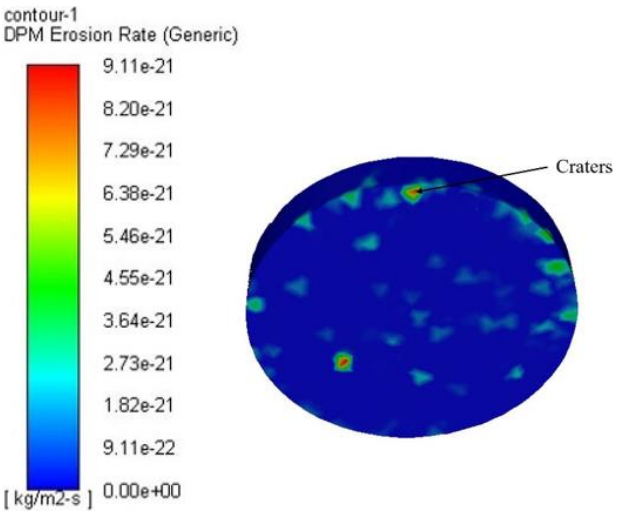


(a)

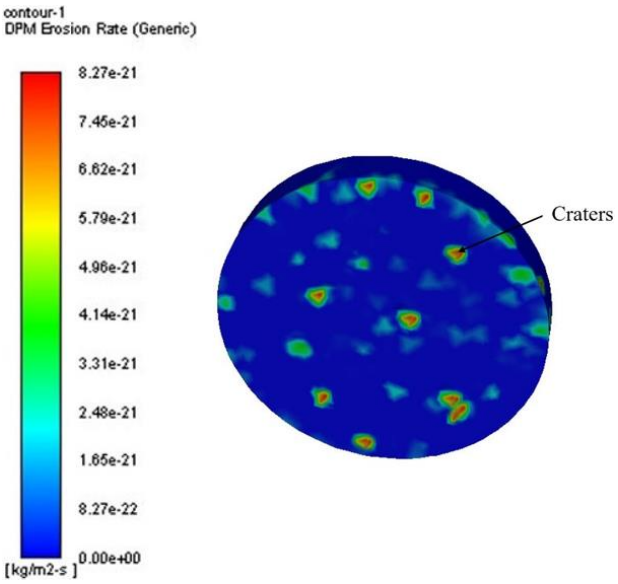


(b)

**Fig**. 4. Erosion rate without silicon carbide (a) and with silicon carbide (b).

Figure 4 serves as compelling visual evidence of the transformative influence of silicon carbide on the EDM process. By elucidating the stark contrast in erosion rates between scenarios with and without silicon carbide, this figure underscores the pivotal role played by silicon carbide particles in optimizing machining performance and achieving superior surface quality in EDM applications. The presence of silicon carbide particles not only promotes stable discharge conditions but also helps in averting arcing, contributing to uniform material removal from the workpiece.

The results presented in Figure 4 are based on a comprehensive thermoelectrical model integrated with computational fluid dynamics (CFD) and erosion models. EDM, being inherently a thermoelectrical process, necessitates the coupling of heat transfer mechanisms with the fluid dynamics and material erosion phenomena. The governing equations for the heat transfer model are based on the principles of conduction, convection, and radiation within the workpiece and tool materials. The heat generated by the electrical discharges is modeled using the Joule heating effect, where the local temperature rise due to the electric current leads to material melting and vaporization. This thermal model is coupled with a CFD model that simulates the flow of the dielectric medium, including the dispersion and interaction of silicon carbide particles. The erosion model calculates the rate of material removal based on the thermal energy input and the resulting phase changes in the material. The integration of these models allows for a detailed simulation of the EDM process, capturing the intricate interplay between electrical discharge, heat transfer, fluid dynamics, and material erosion. The presence of silicon carbide particles is modeled to enhance the electrical discharge stability and improve heat dissipation, leading to more uniform and efficient material removal. This comprehensive modeling approach provides a robust framework for understanding and optimizing the EDM process, as evidenced by the results shown in Figure 4.

### 3.4. Powder and debris particle interaction

Discrete Phase Modeling (DPM) is utilized at the Inter-Electrode Gap (IEG) to investigate the trajectory of fragmented particles. The ANSYS FLUENT software employs the Euler-Lagrange technique to implement the Lagrangian discrete phase model, with the parameters utilized for simulating particles detailed in Table 4. Within this modeling framework, the continuous medium of the fluid phase, referred to as the primary phase, is analyzed by solving the Navier-Stokes equations. Conversely, the dispersed phase, known as the secondary phase, is managed by tracking multiple particles within the computed flow field. This dispersed phase is capable of transferring momentum, mass, and energy to the fluid phase. The proportion of the dispersed phase in relation to the fluid phase typically remains between 10% and 12%. The trajectory of a discrete phase particle is determined by integrating the force equilibrium on the particle within the Lagrangian reference frame. The equation that represents the equilibrium of forces per unit mass of the particle is as equation (2):

$$\frac{du_p}{dt} = \mathrm{FD}\left(\vec{u} - \overrightarrow{u_p}\right) + \frac{\vec{g}\left(\rho_p - \rho\right)}{\rho_p} + \vec{F} \quad (2)$$

Here, $(\frac{du_p}{dt})$ represents the net particle inertia, incorporating the effects of acceleration over time. On the right side of the equation, FD denotes the drag force experienced by the particle due to its motion relative to the surrounding fluid, while g accounts for the gravitational force acting on the particle. Additionally, ρp and ρ represent the densities of the particle and fluid, respectively, with F encompassing any additional external forces exerted on the particle.

This investigation entails the injection of particles with a spherical morphology from the work surface, followed by a detailed analysis of their trajectory and behavior within the machining environment. The introduced powder particles navigate through the inter-electrode gap (IEG), potentially adhering to either the workpiece or the tool's surface. It is crucial to note that the presence of powder particles significantly influences the overall machining process.

The injected powder particles serve several critical functions in the machining process. Firstly, they facilitate the establishment of a conductive path within the IEG, essential for sustaining electrical discharge and promoting material removal from the workpiece. Secondly, these particles contribute to the formation of a stable plasma channel, mitigating the occurrence of undesirable phenomena such as arcing and electrode wear. Moreover, the powder particles aid in enhancing the flushing action within the machining zone, effectively removing debris and

maintaining a conducive environment for efficient material removal. The trajectory and behavior of powder particles play a vital role in shaping the dynamics of the machining process. Their presence influences various aspects of machining performance, including material removal efficiency, surface quality, and electrode wear. As such, understanding and optimizing the behavior of powder particles is essential for enhancing the effectiveness and reliability of electrical discharge machining operations.

Discrete phase modeling (DPM) is employed to explore the trajectory of fragmented particles within the IEG. Utilizing the Euler-Lagrange technique, the DPM model tracks particle movements, considering forces such as drag force, gravity, and additional forces. The injected powder particles traverse the gap, potentially adhering to the workpiece or tool surface, and play a crucial role in the machining process.

Figures 5a, b, and c offer a comprehensive visualization of the intricate interplay between powder particles, burnt remnants, and the resultant craters, shedding light on their dynamic interactions within the powder-mixed Electrical Discharge Machining (PMEDM) environment. These visual representations encapsulate crucial stages of the machining process and elucidate the pivotal role played by powder particles in shaping the machining dynamics.

(a) Initial Stage

At the outset, as depicted in Figure 5a, the particles assume their initial positions within the dielectric medium before any electrical discharge is initiated. This stage serves as a precursor to the machining operation, showcasing the uniform distribution of powder particles throughout the medium.

(b) Single Spark and 2 gm/lit P.C.

Figure 5b delves into the trajectory of particles amidst a single spark event, featuring a powder concentration of 2 gm/lit. As the electrical discharge commences, the powder particles undergo energization, exhibiting a characteristic zigzag motion within the confines of the inter-electrode gap (IEG). Under the influence of electric forces, these particles organize themselves into chains within the sparking region, fostering conditions conducive to stable discharge phenomena.

(c) Multiple Spark and 4 gm/lit P.C

In Figure 5c, the trajectory of particles amidst multiple spark events unfolds, accompanied by a heightened powder concentration of 4 gm/lit. With the escalation in discharge frequency, the particles experience intensified movement and aggregation within the IEG. The augmented presence of powder particles induces alterations in the plasma channel, engendering a more uniform distribution of discharge energy across the workpiece surface. Consequently, this engenders consistent erosion patterns on the workpiece surface, contributing to enhanced material removal efficiency.

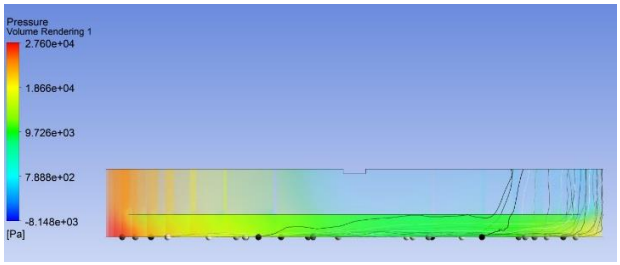


(a)

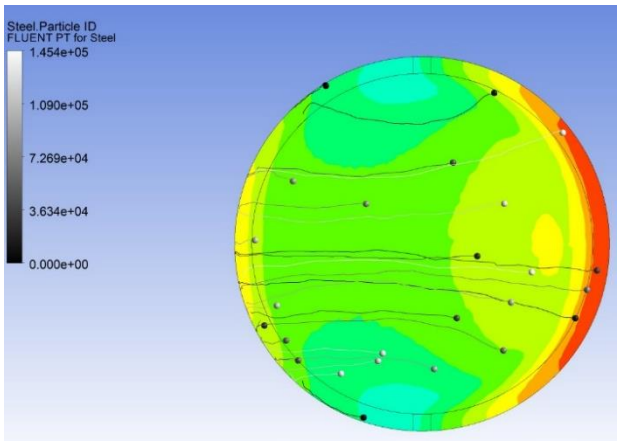


(b)

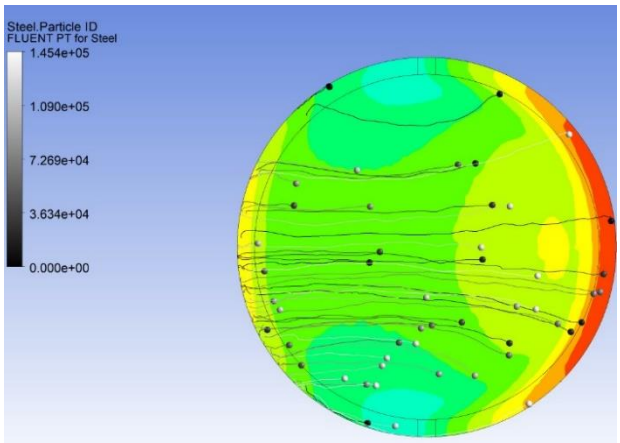


(c)

**Fig. 5.** Initial stage (a) Single Spark and 2 gm/lit P.C. (b) and Multiple spark and 4 gm/lit P.C (c) of particles trajectory.

Figure 5 serves as a valuable analytical tool, offering nuanced insights into the behavior of powder particles at distinct stages of the PMEDM process. By elucidating the intricate dynamics governing particle trajectories and their influence on discharge phenomena, these visual representations underscore the pivotal role played by powder particles in optimizing machining performance and efficiency.

The effect of powder concentration on the material removal rate (MRR) is a pivotal consideration in the investigation. As powder concentration fluctuates, discernible alterations in material removal efficiency arise during the machining process. Statistical validation of these trends is provided through analysis of variance (ANOVA), elucidating the extent to which powder concentration impacts MRR. Hypothetically, heightened powder concentrations foster a more conductive milieu within the inter-electrode gap, thereby fostering stable discharge and amplifying material removal efficiency. By amalgamating empirical observations, statistical scrutiny, theoretical discourse, and computational simulations, the study furnishes a comprehensive comprehension of how powder concentration influences MRR in powder-mixed electro-discharge machining (PMEDM) processes. The ramifications of this observed relationship for industrial applications are discussed, offering insights for manufacturers and practitioners to optimize powder concentration levels in PMEDM setups, consequently enhancing machining efficiency and productivity.

## 4. CONCLUSIONS

Through a comprehensive investigation encompassing rigorous discussion, experimental work, and software-based analysis, the following key conclusions are drawn:

- The concentration of silicon carbide powder significantly enhances Material Removal Rate (MRR) in powder-mixed Electrical Discharge Machining (PMEDM). On average, there is an 11% improvement in MRR compared to processes conducted without powder particles, showcasing the pivotal role of powder concentration in machining efficiency.
- The simulation results of MRR exhibit commendable agreement with experimental findings, validating the efficacy of computational fluid dynamics (CFD) in predicting machining performance accurately. This alignment underscores the reliability and predictive capability of simulation techniques in optimizing PMEDM processes.
- The interaction between powder particles and debris movement within the inter-electrode gap (IEG) provides valuable insights into the trajectory of debris particles, particularly facilitated by the flushing system. Understanding this interaction aids in devising strategies to mitigate debris accumulation and optimize machining conditions.
- The efficacy of a robust flushing system in renovating the IEG and preventing arcing is demonstrated, resulting in a tangible improvement in MRR. Effective flushing mechanisms are essential in maintaining stable discharge conditions and enhancing machining efficiency by minimizing interruptions caused by debris accumulation.
- Eddies generated in the dielectric medium due to the stirrer mechanism serve as a secondary stirring mechanism, mitigating the redeposition of debris on the machined surface. This secondary stirring action ensures the removal of debris particles from the machining zone, contributing to improved surface quality and enhanced MRR.

## REFERENCES

[1] H. Q. Nguyen et al., "Influence of PMEDM Factors on Surface Roughness When Processing SKD11 Steel", in *Lecture notes in networks and systems*, 2022, pp. 536–544. doi: 10.1007/978-3-030-92574-156.

[2] H. Q. Nguyen et al., "Multi-objective Optimization of PMEDM Process for Minimum Surface Roughness and Maximum Material Removal Speed When Processing SKD11 Steel", *in Lecture notes in networks and systems*, 2022, pp. 634–644. doi: 10.1007/978-3-030-92574-1_66.

[3] B. Surekha, T. S. Lakshmi, H. Jena, and P. Samal, "Response surface modelling and application of fuzzy grey relational analysis to optimise the multi response characteristics of EN-19 machined using powder mixed EDM," *Australian Journal of Mechanical Engineering*, vol. 19, no. 1, pp. 19–29, Jan. 2019, doi: 10.1080/14484846.2018.1564527.

[4] A. Y. Joshi and A. Y. Joshi, "A systematic review on powder mixed electrical discharge machining", *Heliyon*, vol. 5, no. 12, p. e02963, Dec. 2019, doi: 10.1016/j.heliyon.2019.e02963.

[5] M. Kolli and A. Kumar, "Effect of dielectric fluid with surfactant and graphite powder on Electrical Discharge Machining of titanium alloy using Taguchi method," *Engineering Science and Technology an International Journal*, vol. 18, no. 4, pp. 524–535, Dec. 2015, doi: 10.1016/j.jestch.2015.03.009.

[6] S.-F. Ou and C.-Y. Wang, "Effects of bioceramic particles in dielectric of powder-mixed electrical discharge machining on machining and surface characteristics of titanium alloys," *Journal of Materials Processing Technology*, vol. 245, pp. 70–79, Jul. 2017, doi: 10.1016/j.jmatprotec.2017.02.018.

[7] G. Talla, D. K. Sahoo, S. Gangopadhyay, and C. K. Biswas, "Modeling and multi-objective optimization of powder mixed electric discharge machining process of aluminum/alumina metal matrix composite," *Engineering Science and Technology an International Journal*, vol. 18, no. 3, pp. 369–373, Sep. 2015, doi: 10.1016/j.jestch.2015.01.007.

[8] V. D. Bui, J. W. Mwangi, and A. Schubert, "Powder mixed electrical discharge machining for antibacterial coating on titanium implant surfaces," *Journal of Manufacturing Processes*, vol. 44, pp. 261–270, Aug. 2019, doi: 10.1016/j.jmapro.2019.05.032.

[9] F. Modica, V. Marrocco, M. Valori, F. Viganò, M. Annoni, and I. Fassi, "Study about the Influence of Powder Mixed Water Based Fluid on Micro-EDM Process," *Procedia CIRP*, vol. 68, pp. 789–795, Jan. 2018, doi: 10.1016/j.procir.2017.12.156.

[10] M. P. Mughal *et al.*, "Surface modification for osseointegration of Ti6Al4V ELI using powder mixed sinking EDM," *Journal of the Mechanical Behavior of Biomedical Materials/Journal of Mechanical Behavior of Biomedical Materials*, vol. 113, p. 104145, Jan. 2021, doi: 10.1016/j.jmbbm.2020.104145.

[11] S. A. Mullya and G. Karthikeyan, "Comparative Study of dielectric and Debris flow in Micro-Electrical Discharge Milling Process using cylindrical and Slotted tools," in *Lecture notes on multidisciplinary industrial engineering*, 2019, pp. 17–26. doi: 10.1007/978-981-32-9471-4_2.

[12] S. Mullya and G. Karthikeyan, "Dielectric flow observation at inter-electrode gap in micro-electro-discharge-milling process," *Proceedings of the Institution of Mechanical Engineers Part B Journal of Engineering Manufacture*, vol. 232, no. 6, pp. 1079–1089, Aug. 2016, doi: 10.1177/0954405416662082.

[13] V. Ganachari, U. Chate, L. Waghmode, P. Jadhav, S. Mullya, and N. Prasad, "Simulation and experimental investigation of performance characteristics of dry and near dry EDM process," *Advances in Materials and Processing Technologies*, vol. 8, no. 3, pp. 3013–3028, Aug. 2021, doi: 10.1080/2374068x.2021.1945296.

[14] S. Srivastava, M. Vishnoi, M. T. Gangadhar, and V. Kukshal, "An insight on Powder Mixed Electric Discharge Machining: A state of the art review," *Proceedings of the Institution of Mechanical Engineers Part B Journal of Engineering Manufacture*, vol. 237, no. 5, pp. 657–690, Jul. 2022, doi: 10.1177/09544054221111896.

[15] A. Schubert, V. D. Bui, I. Schaarschmidt, T. Berger, and A. Martin, "Developments in Powder Mixed EDM and its perspective Application for targeted Surface Modification," *Procedia CIRP*, vol. 113, pp. 100–119, Jan. 2022, doi: 10.1016/j.procir.2022.09.134.

[16] S. S. Shirguppikar and M. S. Patil, "Experimental investigation on micro-electro discharge machining process using tungsten carbide and titanium nitride-coated micro-tool electrode for machining of Ti-6Al-4V," *Advances in Materials and Processing Technologies*, vol. 8, no. sup1, pp. 187–204, Oct. 2020, doi: 10.1080/2374068x.2020.1833399.

[17] S. Shirguppikar *et al.*, "Assessing the effects of uncoated and coated electrode on response variables in electrical discharge machining for TI-6AL-4V titanium alloy," *Tribology in Industry*, vol. 43, no. 4, pp. 524–534, Dec. 2021, doi: 10.24874/ti.1020.12.20.03.